This is a repository copy of *The role of particle contact in densification of FLASH sintered potassium sodium niobate*.

White Rose Research Online URL for this paper:
https://eprints.whiterose.ac.uk/165122/

Version: Accepted Version

Article:
Serrazina, R., Senos, A.M.O.R., Pereira, L. et al. (3 more authors) (2020) The role of particle contact in densification of FLASH sintered potassium sodium niobate. European Journal of Inorganic Chemistry, 2020 (39). pp. 3720-3728. ISSN 1434-1948

https://doi.org/10.1002/ejic.202000458

This is the peer reviewed version of the following article: Serrazina, R., Senos, A.M.O.R., Pereira, L., Dean, J.S., Reaney, I.M. and Vilarinho, P.M. (2020), The Role of Particle Contact in Densification of FLASH Sintered Potassium Sodium Niobate. Eur. J. Inorg. Chem., which has been published in final form at https://doi.org/10.1002/ejic.202000458. This article may be used for non-commercial purposes in accordance with Wiley Terms and Conditions for Use of Self-Archived Versions.

Reuse
Items deposited in White Rose Research Online are protected by copyright, with all rights reserved unless indicated otherwise. They may be downloaded and/or printed for private study, or other acts as permitted by national copyright laws. The publisher or other rights holders may allow further reproduction and re-use of the full text version. This is indicated by the licence information on the White Rose Research Online record for the item.

Takedown
If you consider content in White Rose Research Online to be in breach of UK law, please notify us by emailing eprints@whiterose.ac.uk including the URL of the record and the reason for the withdrawal request.

eprints@whiterose.ac.uk
https://eprints.whiterose.ac.uk/

(paper accepted in European Journal of Inorganic Chemistry, August 2020)
(Invitation for a special issue for CICECO – Aveiro Materials Institute)
doi.org/10.1002/ejic.202000458

The role of particle contact in densification of FLASH sintered Potassium Sodium Niobate

Ricardo Serrazina[1], Ana M. O. R. Senos[1*], Luis Pereira[2], Julian S. Dean[3], Ian M. Reaney[3], Paula M. Vilarinho[1*]

[1] Department of Materials and Ceramic Engineering, CICECO – Aveiro Materials Institute, University of Aveiro, 3810-193 Campus Santiago, Portugal
[2] CENIMAT-I3N, School of Science and Technoloy, FCT-NOVA, Universidade NOVA de Lisboa, Campus da Caparica. 2829-516 Caparica, Portugal
[3] Materials Science and Engineering, University of Sheffield, Sheffield S1 3JD, UK.

*Correspondent authors: anamor@ua.pt, paula.vilarinho@ua.pt

Academic titles and personal URLs:
Mr. Ricardo Serrazina
http://www.ciceco.ua.pt/index.php?menu=221&language=eng&tabela=pessoaldetail&user=1215
Prof. Ana M. O. R. Senos
http://www.ciceco.ua.pt/index.php?tabela=pessoaldetail&menu=218&user=390
Prof. Luis Pereira
https://www.cenimat.fct.unl.pt/people/luis-miguel-nunes-pereira
Dr. Julian S. Dean
https://www.sheffield.ac.uk/materials/people/academic-staff/julian-dean
Prof. Ian M. Reaney
https://www.sheffield.ac.uk/materials/people/academic-staff/ian-reaney
Paula M. Vilarinho
http://www.ciceco.ua.pt/index.php?tabela=pessoaldetail&menu=218&user=477

Institution twitter account:
https://twitter.com/ciceco_ua

Abstract

Potassium sodium niobate, $K_{0.5}Na_{0.5}NbO_3$ (KNN) is a lead-free piezoelectric with the potential to replace lead zirconate titanate (PZT) in electromechanical applications. Due to its cuboid particle morphology and volatile elements, monophasic and dense ceramics are difficult to obtain via conventional sintering. In this work, isothermal FLASH sintering produced uniformly densified KNN ceramics at 900 ºC, 200 ºC lower than conventional sintering. Specific surface area (SSA) analysis of *pre-FLASH* ceramics revealed that a 30 min isothermal hold at 900 ºC, before the application of electric field, increased the contact area between particles and was crucial to promote uniform densification. Finite element modelling (FEM) revealed why density is more uniform when using isothermal heating compared with a constant heating rate, commonly used in FLASH sintering. These results extend our understanding of FLASH sintering and illustrate its relevance for the development of lead-free piezoelectrics.

Key words: FLASH sintering, potassium sodium niobate, KNN, isothermal, Finite Element Modelling, lead-free piezoelectrics

Table of contents

Key words: FLASH sintering; ceramics; sintering

This work is about the FLASH sintering process and respective operating sintering mechanisms in lead-free piezoelectrics, namely, in $K_{0.5}Na_{0.5}NbO_3$, KNN. Our study reveals the importance of pre-FLASH microstructure for the engineering of uniform, highly dense ceramics by FLASH. We show that isothermal steps, before the application of the electric field, induce a higher degree of densification on FLASH sintered KNN.

Introduction

Potassium sodium niobate, $K_{0.5}Na_{0.5}NbO_3$ (KNN), is a promising lead free piezoelectric but it is difficult to densify by conventional sintering due to alkali volatilization (K and Na) at T > 1100 ºC [1], [2]. Further knowledge of the influence of ceramic processing on the fabrication of stoichiometric KNN is therefore, crucial if it is to replace $Pb(Zr_{1-x}Ti_x)O_3$ (PZT) [2]. KNN presents a relatively low piezoelectric coefficient when compared with PZT, however, a significantly higher transition temperature (ca. 420 ºC) [3]. Piezoelectric properties of KNN may be increased (up to 650 pC/N) if what was described as a New Phase Boundary (NPB) is constructed [4], or by doping [5], similarly to what was done for PZT.

However, the processing of KNN needs to be improved to realize homogenous ceramics with optimised, reliable and thermally stable electromechanical properties. Within this context, alternative sintering techniques have been developed, many of which exhibit lower thermal budgets than conventional methods. Among such methods, FLASH is capable of sintering a wide variety of ceramics at significantly lower temperature and time than conventional processes [6]–[8].

FLASH is a very fast, low-temperature, sintering technique, in which an electric field is directly applied to a green body. At a specific combination of electric field, temperature and/or atmosphere, densification occurs in a short period of time, typically a few seconds (≤ 60 s) [7]. The mechanism of FLASH sintering depends on the material, but is typically associated with thermal runaway promoted by Joule heating [9], [10]. The electric field induces defect migration, most probably through grain boundaries, that often contain a transient liquid phase that also permits particles to slide, further aiding densification [11]. The speed of FLASH sintering is a crucial factor to promote densification. However, the net microstructure is far from equilibrium, with a high probability of inhomogeneous densification, grain growth and properties [12], [13]. Consequently, microstructural heterogeneities become problematic for larger and geometrically complex specimens [6], [14]. In a typical FLASH process, a constant electric field is applied directly to the ceramic, along with a constant heating rate step. When the material becomes sufficiently conductive, FLASH

occurs, with a rapid increase of current density and shrinkage at which point current flow must be limited to avoid melting [7], [15].

When performed as described above, FLASH is designated as a Constant Heating Rate (C.H.R.) process, with three different stages: I) incubation, II) FLASH event and III) steady-state [16]. However, isothermal conditions (I.C.) may be used at the so-called FLASH temperature, for which the electric field is applied after a dwell time. After the application of the electric field, incubation allows the current to flow and FLASH to occur, followed by the same three stages mentioned above. The result is, typically, a higher degree of densification and a more uniform microstructure in comparison with C.H.R. FLASH [7], [17]. Recently, it has been reported that the degree of densification and uniformity can be further improved when current density is monitored and increased with a constant rate, either in C.H.R. or I.C. [18], [19].

Several research groups have already reported the densification of KNN [10], [20], [21]. Furthermore, a reactive-FLASH process has been used to produce monophasic KNN from a 50 mol.% mixture of $KNbO_3$ and $NaNbO_3$ [22]. Initial studies reported that dog-bone shaped KNN ceramics may be FLASH sintered in 30 s to 94% theoretical density at 990 ºC under 50 V/cm and 20 mA/mm^2. It was postulated that a core-shell of Na-K was formed to account for preferential heating at particle surfaces and Na volatilization [20].

Recently, we have suggested that current flow through grain boundaries is a possible mechanism for the FLASH densification of KNN, resulting in amorphization and particle sliding [10], [21]. Despite these advances, it remains unclear how to control the shrinkage. Moreover, if our theory is correct, then *pre-FLASH* microstructure, i.e., the green pellet particle-particle contacts and arrangement, must have an influence on the shrinkage uniformity and specimen final density.

In this work therefore, we have used different cycles (C.H.R. and I.C.) to produce KNN by FLASH to identify the influence of an isothermal step prior to the application of an electric field. Beyond the expected thermal uniformity, we propose that the isothermal step allows neck formation and particle contact uniformity, which triggers a more controlled and homogeneous current density distribution, ultimately leading to improved densification and microstructure.

Finite Element Modelling (FEM) simulations provide key information on current flow through isothermally and non-isothermally heated KNN.

Experimental

Ultra-high purity alkali carbonates (K_2CO_3, Sigma-aldrich, 99.99% and Na_2CO_3, Sigma-aldrich, 99.999%) and niobium oxide (Nb_2O_5, Alfa Aesar, 99.9%) were weighed and mixed to produce $K_{0.5}Na_{0.5}NbO_3$ powders by a conventional solid-state route. Detailed information on powder preparation and characterization may be found in supplementary information. Green compacts (ca. 15 x 5 x 2 mm^3) were uniaxially (130 MPa) and isostatically (250 MPa) pressed, to 65 $\pm$ 2 % green density. After pressing, pellets were conventionally and FLASH sintered in a horizontal adapted dilatometer, using a contacting alumina rod to record shrinkage, with a sensor spring force of 1.4 N. All sintering steps (both FLASH and conventional) were performed in air, with constant heating and cooling rates of 10 ºC/min. Conventional sintering was performed at 1100 ºC for 1 h.

Constant heating rate (C.H.R.) FLASH experiments were performed at 300 V/cm DC electric field applied through two opposite platinum sheets. The power supply (*EPS HV 5006-400*) was automatically switched from voltage to current control when the limit of 20 mA/mm^2 was reached. The limited current was kept for 60 s and the furnace cooled after the FLASH.

Isothermal condition (I.C.) FLASH was performed without any applied electric field until the furnace reached 900 ºC. At such temperature, a 30 min dwell was employed, and the 300 V/cm electric field was applied after the isothermal step. Following an incubation time, the pellets FLASH sintered with similar conditions of limiting current to C.H.R. FLASH. Table 1 shows the thermal cycle and FLASH conditions of the different sintering experiments in this work.

Table 1 - Sintering experimental conditions used in this work to sinter KNN ceramics by conventional and FLASH processes.

Specimen		Heating/ cooling rate (ºC/min)	$T_{Furnace-max}$ (ºC)	Isothermal time (min) (at T_{max})	Electric field (V/cm)	Current density (mA/mm^2)
Conventional		10 ºC/min	1100	60	0	0
FLASH	**C.H.R.**		900	0	300	20
	I.C.		900	30	300	20

During the sintering experiments, the specimen temperature was recorded with an S-type thermocouple located 5 to 7 mm from the ceramic body. Relative displacement, voltage and current were registered using home-made software, with data acquisition each 1 s. Electric field, current density and power dissipation were calculated from the initial dimensions of green compacts.

To determine the ideal time before FLASH in Isothermal Conditions (I.C. 30 min) and to understand its influence on the particle contacts, KNN green compacts were heated to 900 ºC for 15, 30, 60 and 120 min, without electric field. 900 ºC was chosen as the FLASH temperature (T_F) based on previous C.H.R. experiments. The Specific Surface Area, SSA, of each pre-sintered sample was measured by the Brunauer, Emmett, Teller method, BET (*Micromeritics Gemini 2.0*). A pre-measurement drying step of 12 h at 120 ºC was conducted in nitrogen. Relative densities were estimated considering the geometry of the pellet and the theoretical density of KNN (4.5 g/cm^3).

Scanning and transmission electron microscopy, SEM (*Hitachi SU-70*), TEM (*JEOL JEM 2200-FS)* and STEM (*Hitachi HD-2700*) were used to study the microstructure of dense ceramics. For SEM, polished samples were etched 5 min in 40% vol. HF to reveal the grain structure. The fracture surfaces of thermally treated samples were also inspected by SEM. For TEM, ceramics were polished with diamond paper in a tripod mounting and a Gatan Precision Ion Polishing System (*PIPS)* ion mill was used to obtain electron transparency. A *PANalytical XPERT-PRO* diffractometer, with a copper X-ray source ($K\alpha_1$ = 1.54060 Å), was used to obtain X-ray diffraction (XRD) patterns of KNN powders and crushed

dense ceramics. A step size of 0.026º and accumulation time of 96.39 s was used to acquire XRD data.

COMSOL Multiphysics simulations were carried out to theoretically estimate the current flow and Joule heating as a function of particle contact. Models were based on representative microstructures and SSA results in *pre-FLASH* particle-particle contacts. Simulations were performed as previously reported [10].

Results and discussion

The densification of KNN ceramics was monitored by dilatometry. The length variation as a function of the temperature for conventional, C.H.R. FLASH and I.C. FLASH (30 min at 900ºC) KNN ceramics, is shown in Figure 1. Typical for a ceramic green body, there is an increase in linear shrinkage, corresponding to densification onset, after a minor expansion. Conventionally sintered KNN starts to shrink at ~1000 ºC and the process is completed after 1 h at 1100 ºC with a decrease in length of 13.5%, corresponding to a measured final density of 91%. When an electric field of 300 V/cm is applied along with C.H.R., KNN sinters at T_F (FLASH temperature) ≈ 900 ºC, in agreement with previous work [20]. Approximately 18% shrinkage was achieved after 60 s under current limited conditions and a final furnace temperature of 959 ºC. The total shrinkage of C.H.R. FLASH was higher than that of the conventionally sintered specimen, but its final density was lower (89%). In contrast, when the compacted green ceramic is maintained at 900 ºC for 30 min before the application of the electric field (I.C. FLASH), approximately 14% shrinkage is attained at 942 ºC after sintering. The shrinkage for I.C. FLASH therefore, is similar to that of the conventionally sintered body but the measured total densification is higher (95%) compared with 91% for conventional sintering.

To understand the discrepancies between the dilatometer length shrinkage and density, Table 2 presents the post-sintering shrinkage geometries for all ceramic bodies. At least 3 measurements were taken for each dimension, and an average was considered for calculation. Whereas the shrinkage in radial plan (width x thickness) is near isotropic, it is larger along the length, resulting in discrepancies between the linear shrinkage and measured density. Defining anisotropic shrinkage, f_{as}, as the ratio between the average radial shrinkage,

$((\Delta w/w_0)+(\Delta t/t_0))/2$, and the length shrinkage ($\Delta L/L_0$), f_{as} = 1 is isotropic and anisotropy increases with a decreasing f_{as}. Conventionally sintered ceramics exhibited an anisotropic shrinkage factor f_{as} = 0.6, while that of C.H.R and I.C. FLASH is 0.2 and 0.4, respectively (Table 2). The observed shrinkage anisotropy in contact dilatometry is attributed to the pressure of the displacement sensor, that is more evident when viscous flow sintering occurs [23]. For direct comparison between samples, green compacts of the same dimension and a constant value of initial sensor pressure of 0.15 MPa were utilised. As a result, the net increase in the anisotropy of shrinkage for FLASH sintered ceramics, e.g. C.H.R. sample (f_{as} = 0.2), is directly related to non-uniform densification under an applied electric field, probably associated with viscous flow sintering. Isothermal treatment therefore, prior to the application of the electrical field, created conditions for lower anisotropic shrinkage for FLASH (I.C.) compared with C.H.R. FLASH.

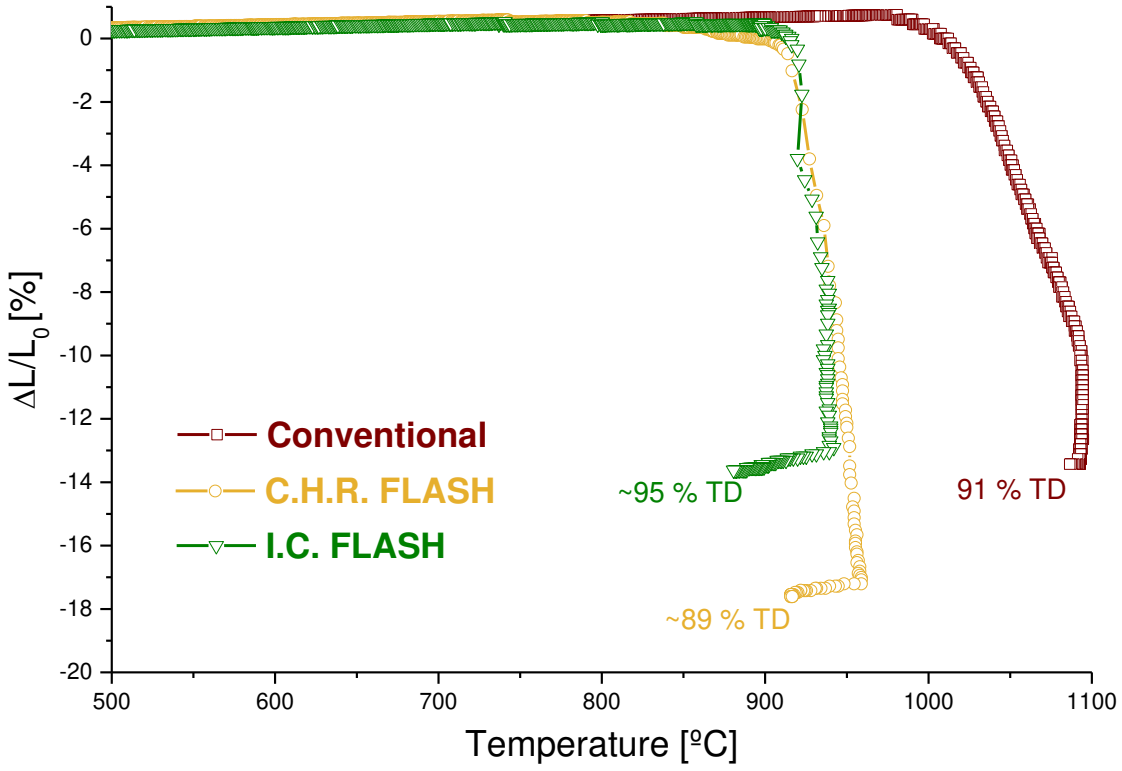

Figure 1 – Relative displacement in length as a function of measured temperature, from green state, for conventional (□), C.H.R. FLASH (○) and I.C. FLASH (30 min at 900ºC FLASH) (▽) specimens. Indications of the electric field (in V/cm), current density (in mA/mm^2) and final densification of ceramics are given.

Table 2 – Post-sintering dimension variation measurements of ceramic bodies in length ($\Delta L/L_0$), width ($\Delta w/w_0$) and thickness ($\Delta t/t_0$), average shrinkage in the three directions ($\Delta S/S_0$) and anisotropic shrinkage (f_{as}) for: conventional, C.H.R. FLASH and I.C. FLASH (30 min at 900ºC).

Ceramic		$\frac{\Delta L}{L_0}$ (%)	$\frac{\Delta w}{w_0}$ (%)	$\frac{\Delta t}{t_0}$ (%)	$\frac{\Delta S}{S_0}$ (%)	f_{as} $\left[\frac{\left(\frac{\Delta w}{w_0}\right)+\left(\frac{\Delta t}{t_0}\right)}{2}\right] / \frac{\Delta L}{L_0}$
Conventional		15.5	8.0	9.5	11.0	0.6
FLASH	**C.H.R.**	22.7	5.1	4.8	10.9	0.2
	I.C. (30 min at 900ºC)	20.6	8.1	7.5	12.1	0.4

To further investigate densification, plots of the furnace temperature are presented in

Figure 2, overlapped with shrinkage behaviour (top graphs), for C.H.R. FLASH (a) and I.C. (30 min at 900 ºC) FLASH (b).

Figure 2 also shows the electric field, current density and power density for C.H.R. (a) and I.C. (b) FLASH. Note that the same x-axis scale (process time) was used for each top and down plot, and t = 0 is FLASH onset in each case. The time scales have different magnitudes for (a) and (b), because of the different experimental setup (C.H.R. and I.C., respectively). The time t = 0 represents the transition between stage I and stage II of FLASH, with the electric field dropping from 300 V/cm and limited to ~50 V/cm, and the current density rising towards its limit (20 mA/mm^2). At this point, power density spikes and the specimen starts to shrink abruptly.

In both cases (C.H.R. (a) and I.C. (b)), stage I of FLASH starts at t ≈ -60 s. This incubation time is observed for C.H.R. (Figure 2a) by a non-linear increase of the power density (and of the current density) with temperature. For I.C. (Figure 2b), stage I starts immediately after the isothermal step when the electric field is applied. Current and power start to increase, and after incubation (60 s), FLASH occurs. Accordingly, for C.H.R. (Figure 2a), temperature increases as stage II is approached in the final seconds of stage I, while in the case of I.C. (Figure 2b), the temperature increase is distributed throughout stage I.

For both ceramics, after stage III (current limited period of 60 s) is completed, the power source is turned off, and shrinkage stops. At this point, the measured final temperatures are ~959 ºC and 942 ºC for C.H.R. (Figure 2a) and I.C. (Figure 2b), respectively.

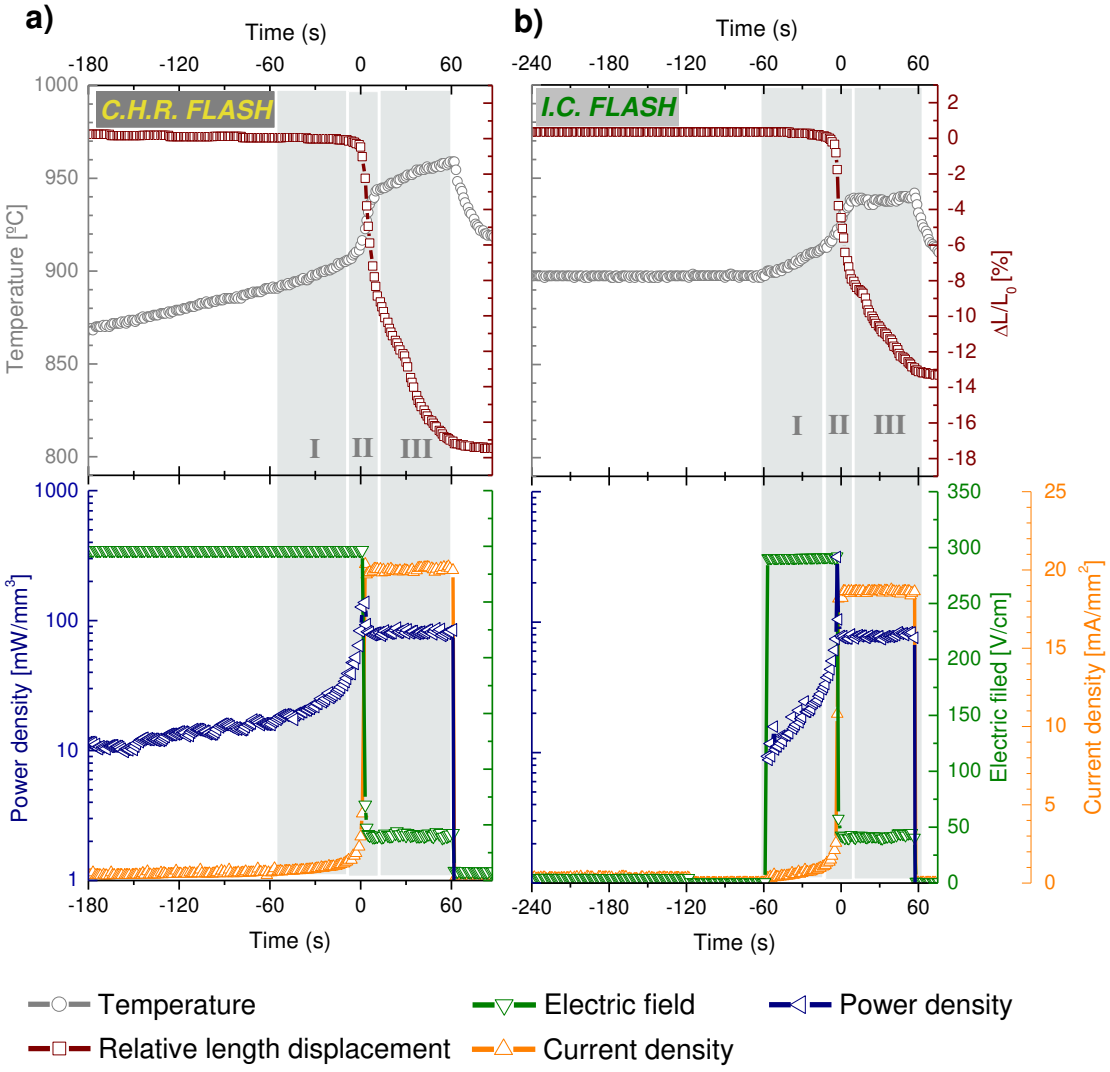

Figure 2 - Simultaneous representation of in-situ measurements (top graphs) of dilatometric behaviour (□), furnace measured temperature (○) and calculated (down graphs) applied electric field (▽), output current density (△) and power density/dissipation (◁) for C.H.R (a) and I.C. (b) FLASH specimens. Each dependence has a correspondent y-axis colour for correct reading. x-axis (time scale) is common for top and bottom graphs, and t = 0 s represents the FLASH event.

From Figure 2, and independent of the thermal cycle used to FLASH sinter KNN, the ceramic body undergoes three typical FLASH stages. The incubation time for both processes (stage I) is similar, implying that the conduction activation mechanism is the same. The increase in temperature is a consequence of thermal runaway with the ceramics dissipating heat to their surroundings. The shrinkage behaviour and temperature increase are markedly different for C.H.R. and I.C. FLASH and are influenced by the compact thermal history. When the electric field is applied along with heating (C.H.R.), the increase in temperature was more abrupt and reached a maximum higher than for I.C. FLASH. In other words, C.H.R. FLASH sintering is faster but less controlled than I.C.

To further analyse the densification of the KNN ceramics (C.H.R. FLASH, I.C. FLASH and conventional), the dependence of the shrinkage derivative with respect to time was calculated and plotted in red in Figure 3. The maximum shrinkage rate of the FLASH processes (C.H.R. (a) and I.C. (b)) is ~10^{-3} s^{-1}. For both FLASH bodies, the maximum shrinkage rate occurred at $t \approx 0$ s, with a pronounced, sharp peak. This peak represents the FLASH onset, with C.H.R. and I.C. FLASH, achieving a shrinkage rate of ~$8x10^{-3}$ s^{-} and ~$5x10^{-3}$ s^{-1}, respectively. Nevertheless, a second densification maximum is observed at $t \approx 30$ s for both, although more evident for C.H.R. In contrast, conventionally sintered KNN exhibits a broader peak, with the maximum shrinkage rate occurring at 1050 ºC. In this case, the maximum shrinkage rate was ca. $1.3x10^{-4}$ s^{-1}, which is more than one order of magnitude lower than that of the FLASH process.

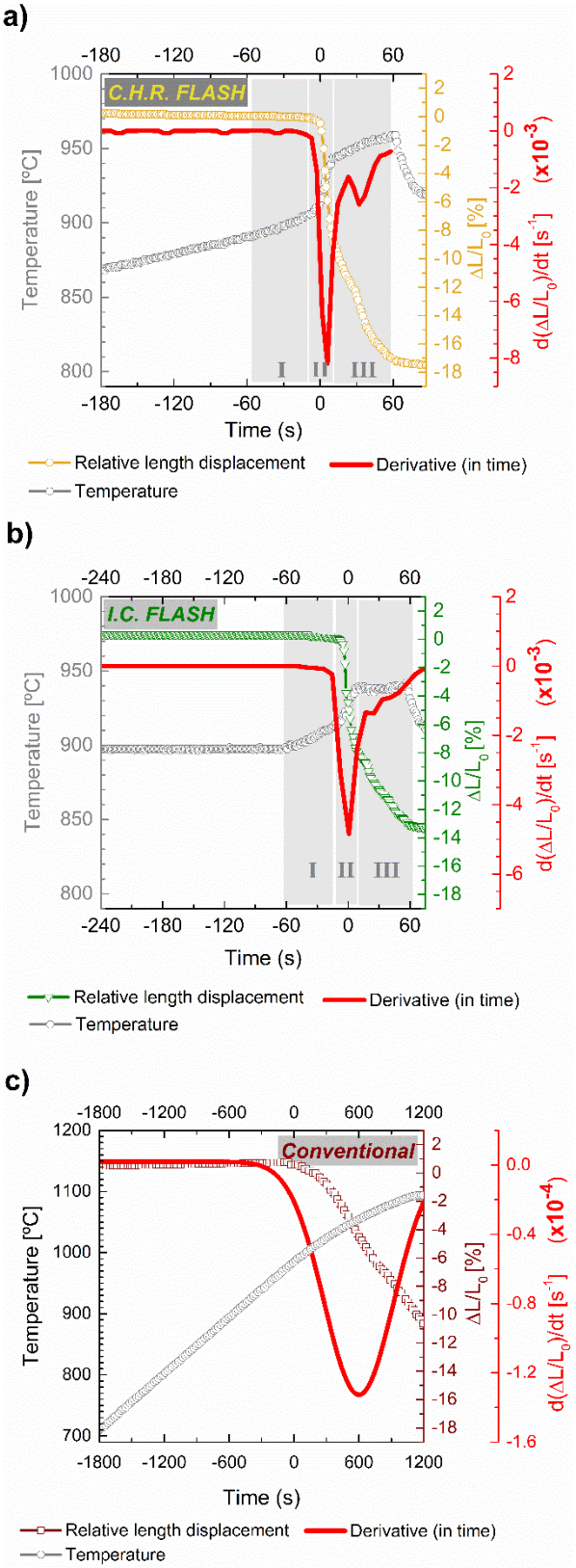

Figure 3 – Relative length variation (shrinkage) derivative as a function of the time (red line), overlapped with relative length variation for each studied KNN pellet, C.H.R. FLASH (a) (○), I.C. (30 min at 900 ºC) FLASH (b) (▽), and conventional (c) (□). For x-axis, t = 0 s represents the onset of FLASH for FLASH ceramics and the beginning of shrinkage for conventional.

The shrinkage rate behaviour for conventional and FLASH suggests that densification in the latter, occurring through viscous flow [21], is significantly faster than that of conventional, but the two FLASH processes are also dissimilar. C.H.R. FLASH (Figure 3a) revealed a higher shrinkage rate than that of I.C. FLASH (Figure 3b). This, together with the higher and more abrupt increase in the measured temperature, revealed that stage II is significantly faster in C.H.R than in I.C. FLASH. The secondary shrinkage rate peak at t ≈ 30 s, more evident in C.H.R., occurs during stage III and may be due to further uncontrolled viscous deformation, that could increase the anisotropic shrinkage. However, a clear understanding of the sintering mechanism associated with the observed secondary shrinkage peak remains to be elucidated.

SEM micrographs (Figure 4 – Scanning electron microscopy (SEM) micrographs of a) C.H.R. FLASH, b) I.C. FLASH and c) conventionally sintered KNN ceramicsFigure 4) confirm that dense KNN ceramics were obtained after sintering for all the three processes, in agreement with calculated densities, and that the cuboid particle shape was maintained. However, a detailed analysis exposes differences in the microstructures, associated with each sintering process. A more defined grain morphology is observed for FLASH ceramics, suggesting preferential chemical attack at grain boundaries of those samples (Figures 4 a) and b)). In conventionally sintered KNN, chemical etching is less preferential in grain boundaries, showing also a worm-like morphology inside the grains. These observations show that the grain boundaries of FLASH and conventionally sintered KNN should be different. On the other hand, more uniform grain size was observed for FLASH sintered ceramics (Figure 4a) and b)), especially for I.C. FLASH. This observation is related with the role of the isothermal step, that promoted a more controlled and uniform densification during FLASH.

To analyse further the microstructures, Transmission Electron Microscopy, TEM, was carried out for I.C. FLASH and conventional ceramics, and representative images are shown in Figure 5a) and b), respectively. Since I.C. FLASH produced uniform density, these ceramics ion thinned more evenly and were further characterized and compared with conventionally sintered KNN.

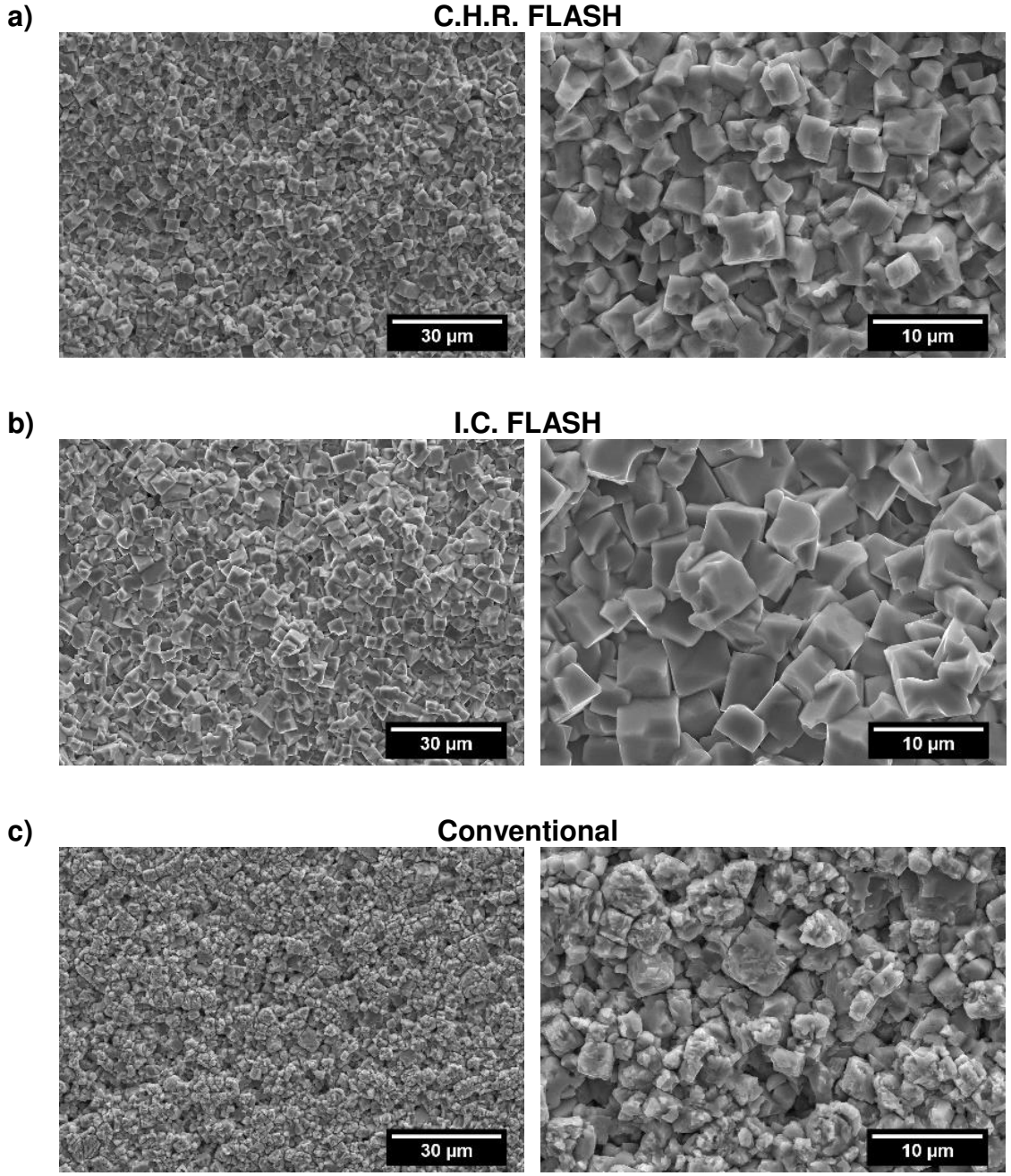

Figure 4 – Scanning electron microscopy (SEM) micrographs of a) C.H.R. FLASH, b) I.C. FLASH and c) conventionally sintered KNN ceramics, acquired with a 15 keV accelerating voltage at different magnifications, 1000 and 3000 times, left and right, respectively.

While conventional ceramic TEM micrographs (Figure 5b) show well defined cuboid grains, with no evidence of particle smoothing or contact melting, FLASH sintered TEM micrographs (Figure 5a) revealed that I.C. FLASH promotes

rounding of KNN cuboid particles (red arrows) and filling of pores and grain boundaries with a glassy phase (green circles). These observations are in agreement with the mechanisms for FLASH sintering KNN presented in Ref [21] and also with the viscous flow FLASH sintering mechanism already refereed.

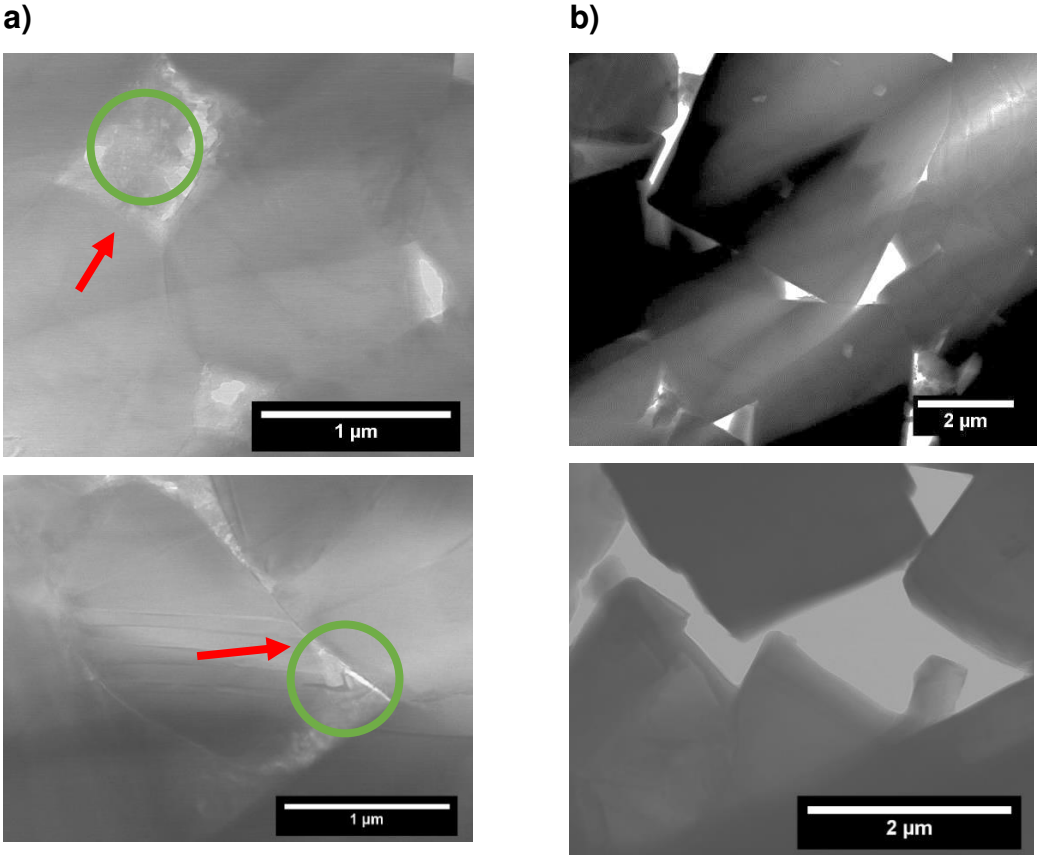

Figure 5 – Transmission electron microscopy micrographs of I.C. FLASH (a) and conventional (b) ceramics.

Despite these microstructural variations, XRD analysis did not reveal any secondary phase or peak broadening. Both FLASH and conventional ceramics are indexed according to a single perovskite structure, corresponding to the $K_{0.5}Na_{0.5}NbO_3$ (JCPDF file 01-085-7128), as shown in Figure 6. Conventional and I.C. FLASH ceramics are similar to KNN powders but the C.H.R. FLASH XRD pattern has less defined maxima and an inversion of the relative intensities of the first and second reflections (2θ ~22.5º and ~32º). This inversion indicates preferential grain orientation in (011) and (100), as observed in KNN thin films [24] and is possibly related to the high degree of shrinkage anisotropy in C.H.R. FLASH.

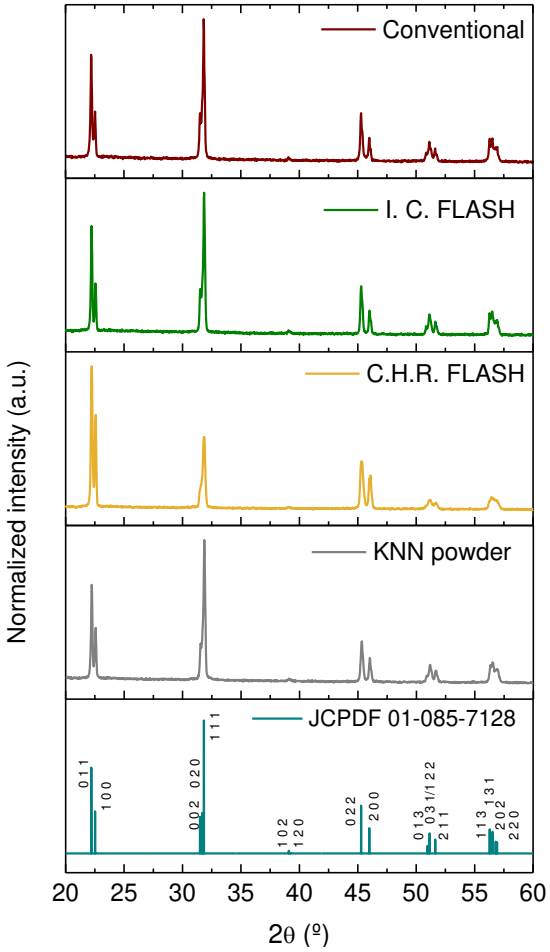

Figure 6 – Normalized X-ray diffraction patterns of KNN powders and sintered ceramics. JCPDF file 01-085-7128 corresponding to the orthorhombic $K_{0.5}Na_{0.5}NbO_3$ pattern is shown for comparison.

Our results provide evidence of densification as well as microstructural and structural differences between C.H.R. and I.C. FLASH, suggesting that the isothermal step has a significant influence. To further investigate the isothermal effect, Specific Surface Area (SSA) analysis by BET and SEM were conducted, as shown in Figure 7. Green KNN pellets were heated up to 900 ºC and isothermal steps (without the application of the electric field) were performed for: 0, 15, 30, 60 and 120 min. After each dwell, in which no significant shrinkage was recorded, pellets were cooled and the SSA of each pellet measured. In parallel, cross section SEM micrographs were collected. Green and isothermal sintered bodies are depicted in Figure 7. The SSA is continuously reduced under the isothermal steps. A decrease from ca. 6.5 m^2/g for the green pellets to ca. 2.3

m^2/g, after 30 min at 900 ºC, corresponding to ~ -64%, was determined and the micrographs clearly show that the isothermal step allowed particles to form necks and continuous contacts (red circles in Figure 7), not present in the green pellets. Longer isothermal periods (60 and 120 min) bring a more modest decrease of SSA and no relevant alterations of the microstructure are visible between 30 and 120 min.

Besides neck growth, particle surface smoothing, not detectable in SEM, is also expected to contribute to the SSA reduction. This SSA reduction, occurring without measurable shrinkage, takes place via non-densifying mass transport, as surface diffusion, typical of the initial stage of sintering in fine powders [25].

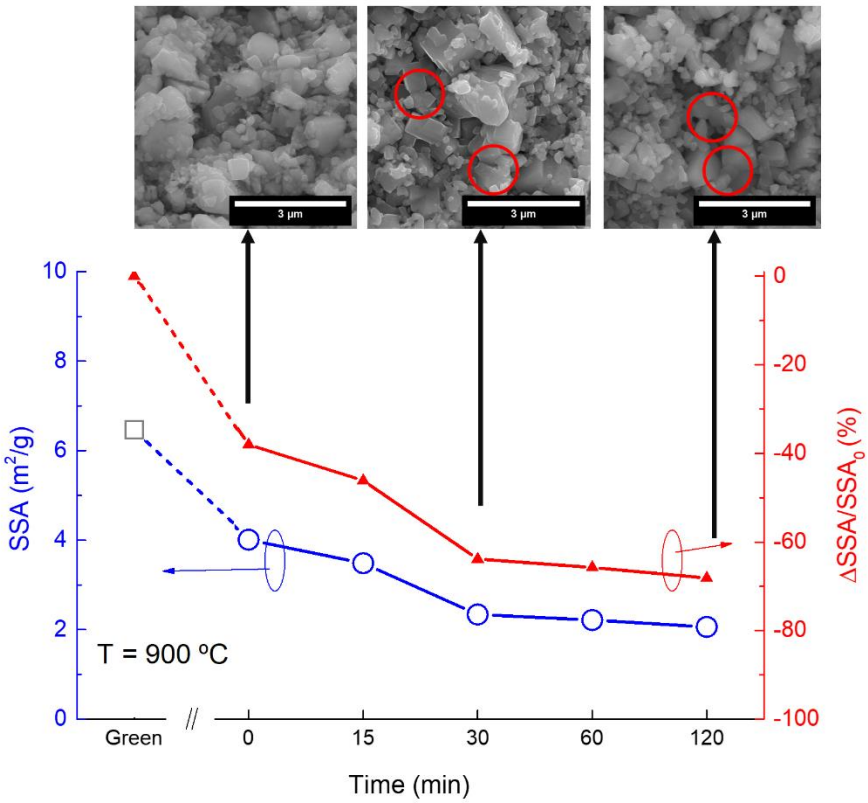

Figure 7 – Specific surface area (SSA) as a function of the tested compact (in blue). Isothermal compacts are identified with blue circles and the green pellet with a grey square. In red, calculated SSA relative variation: $(SSA\text{-}SSA_{Green})/SSA_{Green}$. SEM micrographs of 0, 30 and 120 min isothermal are presented as inset on the graph, respectively from left to right.

We have, thus far, gathered experimental evidence that a 30 min isothermal step promotes uniform particle contact, allowing neck formation and development

of a dense, homogeneous microstructure compared with conventional and C.H.R FLASH KNN. We propose that neck formation permits a more uniform and continuous path for current flow during FLASH, compared with a green body. However, to support this mechanism, the theoretical distribution of the current and respective Joule heating as a function of the particle-particle contact is required. *COMSOL Multiphysics* software was therefore used to model current flow [10].

Two cuboid particles with 1 μm side size were considered to contact in an edge-face [10] configuration. For simplification, only simulations of stage II of FLASH were performed and a conductivity of 1 S/m (measured during FLASH experiments [10]) assigned to each particle. An electric field of 300 V/cm was scaled and applied to the different arrangements of particles. The modelled particles were designed to contact their neighbouring particle by only one face. Considering that each particle has a free-face surface area of 1 μm^2, an increase in contact area of 20, 40 and 60% represents a respective contact area of 0.2, 0.4 and 0.6 μm^2. These percentages of contact area relate to the observed values for SSA (Figure 7) but particle rounding also contributes to SSA and is not accounted for in our current study.

As the contact area increased, the model accounts for neck formation with a neck radius of 0.01 and 0.02 μm introduced for 40 and 60%, respectively. The model specification design is shown in Figure 8, prior to any current and Joule heating simulation.

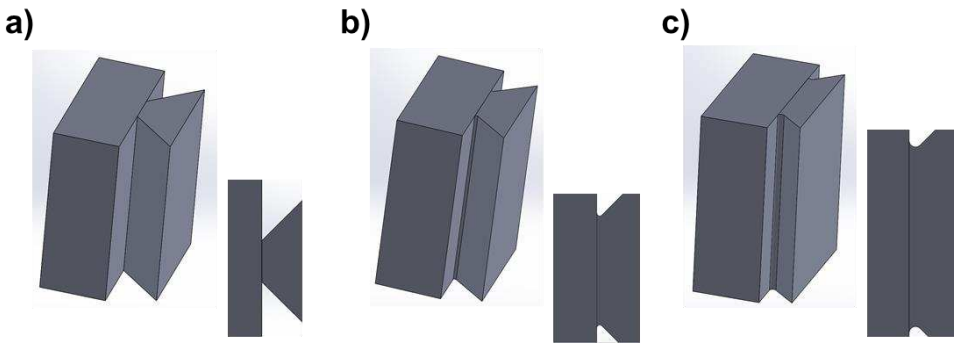

Figure 8 – Model design of particle-particle contact for a 20% (a), 40% (b) and 60% (c) increase in the area contact of a 1 μm^2 cubic face, with representative neck radius increase.

The simulation results for the current density and volumetric electromagnetic losses due to Joule heating, for the three studied particle arrangements, are plotted in Figure 9. A 3D view of the simulated results is presented for each case. Some details of planar views (cut through the middle plane) are also shown, specifically the magnification of the Joule heating distribution for 20 and 60% near the particle contacts (dashed lines). For 20% contact area, a particle-particle, corner-localized current density and Joule heating of approximately 10^2 mA/mm^2 and 10^4 mW/mm^3, respectively, occur. In comparison, with 40% contact area, the maximum current density and Joule heating decrease to, ~ $5x10^1$ mA/mm^2 and $5x10^3$ mW/mm^3, respectively. For 60%, a less localized current density and Joule heating distribution are observed, with maximum values of 10^1 mA/mm^2 and 10^3 mW/mm^3, respectively. These simulations (Figure 9) reveal that both the maximum values and the localization of current flow (with consequent heating) decrease as the particle area contact and neck radius increase.

Comparing the observations from the simulation of current flow and Joule heating with the properties of I.C. FLASH KNN ceramic suggest that the uniform and higher density are a consequence of the increase in particle-particle contact area, with neck formation promoted by the isothermal step at 900 ºC. For C.H.R. FLASH, the sharp contacts promote current localization and the consequent heat generation induces ‘hotspots’ and non-uniform densification.

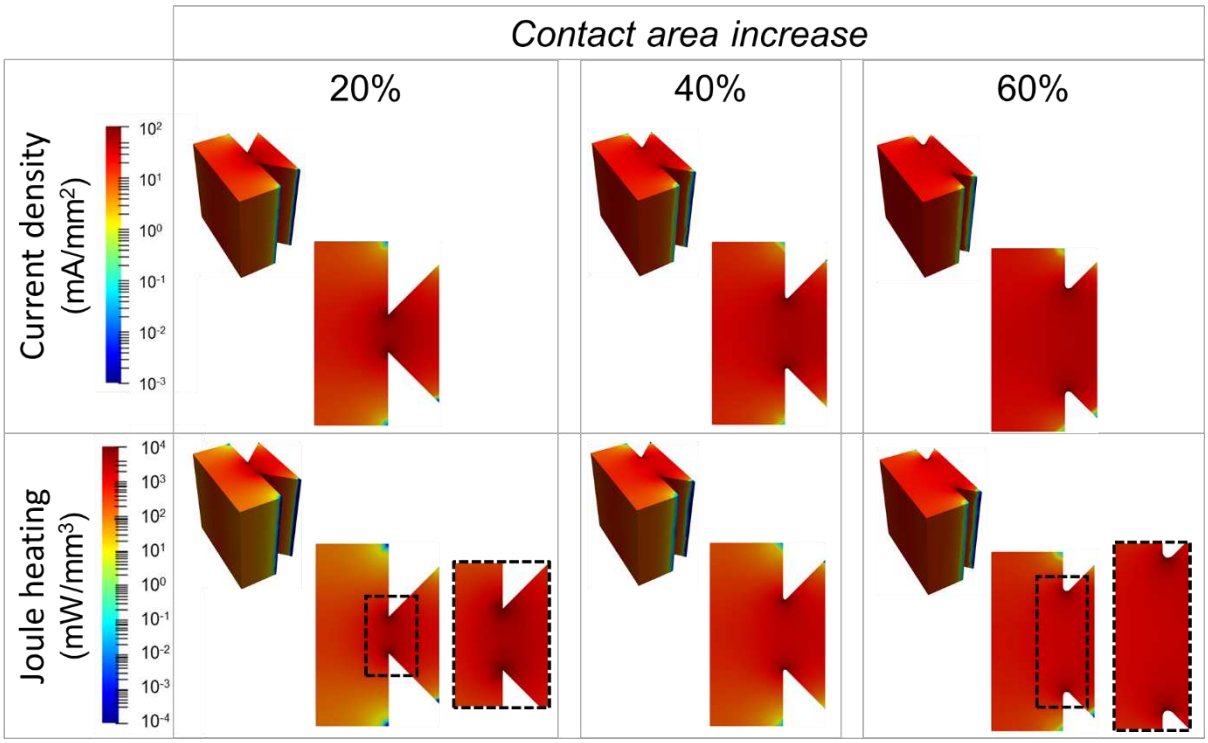

Figure 9 – Representation of the simulations of the current density (top) and Joule heating (down) for the modelled contacting particles with 0.2, 0.4 and 0.6 μm^2 contact area, when subjected to a 300 V/cm and electrical conductivity of 1 S/m.

Conclusions

In conclusion, we have FLASH sintered dense and uniform KNN ceramics in air, at 900 ºC, after a 30 min dwell time, which represents a processing time reduction of 25%, and a maximum temperature decrease of ~20% compared to the conventional processing. Using a combination of isothermal FLASH sintering, and Finite Element Modelling (FEM), we have unveiled the role of particle contact in the densification of FLASH sintered KNN ceramics. The isothermal step allows neck formation, increasing particle contact area and triggering a more uniform and controlled current flow through the body during FLASH. In addition, the anisotropic shrinkage is significantly decreased for I.C. FLASH. The present study reveals that the densification of KNN by FLASH is determined by factors such as electric field, temperature and the *pre-FLASH* microstructure. These observations provide insight into unexplored aspects of FLASH sintered KNN ceramics and highlight its complexity. Such studies are crucial for developing precise control of FLASH sintered materials and can potentially lead to accelerated development of lead free piezoelectrics.

Acknowledgements

This work was also developed within the scope of the project CICECO-Aveiro Institute of Materials, FCT Ref. UID/CTM/50011/2019, financed by national funds through the FCT/MCTES. This work was also financed by Portugal 2020 through European Regional Development Fund (ERDF), in the frame of Operational Competitiveness and Internationalization Programme (POCI), in the scope of the project "FLASH sintering of lead free functional oxides towards sustainable processing of materials for energy and related applications - FLASH", POCI-01-0247-FEDER-029078. Ricardo Serrazina acknowledges FCT for financial support (SFRH/PD/BD/128411/2017).

References

[1] M. E. Villafuerte-Castrejón, E. Morán, A. Reyes-Montero, R. Vivar-Ocampo, J.-A. Peña-Jiménez, S.-O. Rea-López L. Pardo, *Materials*, **2016,** *9*, no. 1, p. 21.

[2] C.-H. Hong, H.-P. Kim, B.-Y. Choi, H.-S. Han, J. S. Son, C. W. Ahn, W. Jo, *J Mater.*, **2016,** *2*, pp. 1–24.

[3] S. Zhang, R. Xia, T. R. Shrout, *J. Electroceramics*, **2007,** *19*, no. 4, pp. 251–257.

[4] X. Lv, J. Zhu, D. Xiao, X. X. Zhang, J. Wu, *Chem. Soc. Rev.*, **2020,** *49*, no. 3, pp. 671–707.

[5] J. Wu, D. Xiao, J. Zhu, *Chem. Rev.*, **2015,** *115*, pp. 2559–2595.

[6] C. E. J. Dancer, *Mater. Res. Express*, **2016,** *3*, no. 10, pp. 102001–102025.

[7] M. Biesuz, V. M. Sglavo, *J. Eur. Ceram. Soc.*, **2019,** *39*, no. 2–3, pp. 115–143.

[8] M. Yu, S. Grasso, R. Mckinnon, T. Saunders, M. J. M. Reece, *Adv. Appl. Ceram.*, **2017,** *116*, no. 1, pp. 1–37.

[9] R. Raj, *J. Eur. Ceram. Soc.*, **2012,** *32*, no. 10, pp. 2293–2301.

[10] R. Serrazina, P. M. Vilarinho, A. M. O. R. Senos, L. Pereira, I. M. Reaney, J. S. Dean, *J. Eur. Ceram. Soc.*, **2020,** *40*, pp. 1205–1211.

[11] R. Chaim, *Scr. Mater.*, **2019,** *158*, pp. 88–90.

[12] W. Qin, H. Majidi, J. Yun, K. van Benthem, *J. Am. Ceram. Soc.*, **2016,** *99*,

no. 7, pp. 2253–2259.

[13] Y. Zhang J. Luo, *Scr. Mater.*, **2015,** *106*, pp. 26–29.

[14] S. Grasso, Y. Sakka, N. Rendtorff, C. Hu, G. Maizza, H. Borodiannska, O. Vasylkiv*J. Ceram. Soc. Japan*, **2011,** *119*, no. 1386, pp. 144–146.

[15] M. Cologna, B. Rashkova, R. Raj, *J. Am. Ceram. Soc.*, **2010,** *93*, no. 11, pp. 3556–3559.

[16] S. K. Jha, K. Terauds, J. Lebrun, R. Raj, *J. Ceram. Soc. Japan*, **2016,** *124*, no. 4, pp. 283–288.

[17] Y. Du, A. J. Stevenson, D. Vernat, M. Diaz, D. Marinha, *J. Eur. Ceram. Soc.*, **2016,** *36*, no. 3, pp. 749–759.

[18] M. K. Punith Kumar, D. Yadav, J. M. Lebrun, R. Raj, *J. Am. Ceram. Soc.*, **2018,** *102*, no. 2, pp. 1–13.

[19] H. Charalambous, S. K. Jha, K. H. Christian, R. T. Lay, T. Tsakalakos, *J. Eur. Ceram. Soc.*, **2018,** *38*, no. 10, pp. 3689–3693.

[20] G. Corapcioglu, M. A. Gulgun, K. Kisslinger, S. Sturm, S. K. Jha, R. Raj, *J. Ceram. Soc. Japan*, **2016,** *124*, no. 4, pp. 321–328.

[21] R. Serrazina, J. S. Dean, I. M. Reaney, L. Pereira, P. M. Vilarinho, A. M. O. R. Senos, *J. Mater. Chem. C*, **2019,** *7*, pp. 14334–14341.

[22] Y. Wu, X. Su, G. An, W. Hong, *Scr. Mater.*, **2020,** *174*, pp. 49–52.

[23] A. R. Boccaccini, *J. Mater. Res.*, **1998,** *13*, no. 6, pp. 1693–1697.

[24] A. Tkach, A. Santos, S. Zlotnik, R. Serrazina, O. Okhay, I. Bdikin, M. E. Costa, P. M. Vilarinho, *Nanomaterials*, **2019,** *9*, no. 11.

[25] S.-J. L. Kang in *Sintering Densification, Grain growth, and Microstructure* (Eds.: S.-J. Kang), Elsevier, **2005**.